Journal of Power Sources 196 (2011) 5679–5684

Contents lists available at ScienceDirect

Journal of Power Sources

journal homepage: www.elsevier.com/locate/jpowsour

Short communication

Preparation of $LiCoPO_4$/C nanocomposite cathode of lithium batteries with high rate performance

The Nam Long Doan, Izumi Taniguchi*

Department of Chemical Engineering, Graduate School of Science and Engineering, Tokyo Institute of Technology, 12-1, Ookayama-2, Meguro-ku, Tokyo 152-8552, Japan

ARTICLE INFO

Article history:
Received 14 January 2011
Received in revised form 16 February 2011
Accepted 17 February 2011
Available online 23 February 2011

Keywords:
$LiCoPO_4$
Nanocomposites
Spray pyrolysis
Lithium-ion batteries
Cathode

ABSTRACT

$LiCoPO_4$/C nanocomposites could be successfully prepared by a combination of spray pyrolysis and wet ball-milling followed by heat treatment. X-ray diffraction analysis confirmed that the $LiCoPO_4$/C nanocomposites were well crystallized in an orthorhombic structure with *Pmna* space group. Scanning electron microscopy and transmission electron microscopy with equipped energy dispersive spectroscopy verified that the $LiCoPO_4$/C nanocomposites were the agglomerates of $LiCoPO_4$ primary particles with a geometric mean diameter of 87 nm, and the carbon was well distributed on the surface of the agglomerates. The $LiCoPO_4$/C nanocomposites were used as cathode active materials for lithium batteries, and the electrochemical tests were carried out for the cell Li|1 M $LiPF_6$ in EC:DMC = 1:1|$LiCoPO_4$/C at various charge–discharge rates. The cells delivered first discharge capacities of 142 and 109 mAh g^{-1} at 0.05 and 20 C, respectively. Furthermore, the discharge capacity after 40 cycles corresponded to 87% of initial one at 0.1 C rate. The excellent rate capability of the cells is mainly due to the well distributed carbon on the $LiCoPO_4$ agglomerates, and a much smaller lithium ion diffusion distance in the electrode.

1. Introduction

The successful development of $LiFePO_4$ as a cathode active material of lithium-ion batteries has promoted strong interest on other transition metal phosphates such as $LiMnPO_4$ and $LiCoPO_4$. Although $LiFePO_4$ is low cost, stable and has excellent rate capability, its working voltage is restricted to approximately 3.5 V versus Li^+/Li [1]. In comparison with $LiFePO_4$, $LiCoPO_4$ presents much higher redox potential at approximately 4.8 V versus Li^+/Li [2], and has the theoretical capacity of 167 mAh g^{-1}. Thus, the theoretical energy density is 1.35 times larger than that of $LiFePO_4$. Its electronic conductivity is less than 10^{-9} S cm^{-1} [3], which is almost similar to that of $LiFePO_4$ and about five orders of magnitude higher than the one of $LiMnPO_4$ [4,5]. Moreover, structure volume change between pristine and delithiated phases is about 2% [6,7], which is much lower than those of $LiFePO_4$/$FePO_4$ (7%) [8] and $LiMnPO_4$/$MnPO_4$ (9%) [9]. This fact may indicate the structure stability of $LiCoPO_4$ during charge/discharge process, thus enhance the cycleability and safety issue of the compound [2]. Due to those advantages, $LiCoPO_4$ could be considered as a candidate for future high voltage cathode materials of lithium-ion batteries.

However, the practical application of $LiCoPO_4$ is still under consideration due to two main reasons: the poor electronic conductivity and the poor compatibility with presently used liquid electrolyte [10,11]. In fact, the poor electronic conductivity is a common problem of lithium transitional metal phosphates [12,13]. For $LiFePO_4$, this weakness has been overcome through conductive layer coating such as carbon [14,15]. However, it was reported that carbon is difficult to be coated on the surface of $LiCoPO_4$ particles [16]. It is suggested that the contact between $LiCoPO_4$ and carbon phases is not as good as the case of $LiFePO_4$.

The preparation of $LiCoPO_4$ cathode material has been done by means of the solid-state reaction [6,7,13,16–28], hydrothermal synthesis [12,29], sol–gel method [16,30–32], co-precipitation [33], optical floating zone method [34], radio frequency magnetron sputtering [35], electrostatic spray deposition technique [36] and microwave heating method [10]. In addition, some approaches have been applied in order to improve the electronic conductivity of the cathode such as carbon coating [16], making composite with carbon [6,7,10,13,20,23,24,37] or divalent cation doping on Li^+ or Co^{2+} site [3,24,28]. However, only few good rate capability results have been reported so far [10].

In our previous work [37], the preparation of $LiMnPO_4$/C nanocomposites was carried out using a combination of spray pyrolysis (SP) and wet ball-milling (WBM) followed by heat treatment. It could be clarified that the $LiMnPO_4$/C nanocomposites

* Corresponding author. Tel.: +81 3 5734 2155; fax: +81 3 5734 2155.
E-mail address: taniguchi.i.aa@m.titech.ac.jp (I. Taniguchi).

0378-7753/$ – see front matter.
doi:10.1016/j.jpowsour.2011.02.039

have the excellent electrochemical performance due to the large specific surface area, the small primary particle size and a well distribution of carbon in the composites. In this study, the combination of SP and WBM followed by heat treatment was applied to the synthesis of $LiCoPO_4$/C nanocomposites, and the physical and electrochemical properties of the $LiCoPO_4$/C nanocomposites were investigated.

2. Experimental

2.1. Precursor solution

The precursor solution was prepared by dissolving the required amounts of $LiNO_3$ (98% purity), H_3PO_4 (85% purity) and $Co(NO_3)_2{\cdot}6H_2O$ (98% purity) in distilled water in a stoichiometric ratio. The concentrations of Li^+, Co^{2+} and PO_4^{3-} were all 0.2 mol dm^{-3}. All chemicals were purchased from Wako Pure Chemical Industries Ltd., Japan.

2.2. Experimental setup and procedure

A schematic diagram and the processing procedure of SP setup were described in our previous paper [38]. SP temperature was 300 °C. As-prepared powders were then milled with acetylene black by WBM. Zirconia balls and a zirconia vial were used in WBM process. Rotating speed and ball-milling time were 800 rpm and 6 h, respectively. Finally, annealing was conducted at 500 °C for 4 h in a N_2 + 3% H_2 atmosphere.

In order to evaluate the carbon composite effect on the physical and electrochemical properties of $LiCoPO_4$/C nanocomposites, $LiCoPO_4$ was prepared by SP at 300 °C followed by heat treatment at 500 °C for 4 h in a N_2 + 3% H_2 atmosphere.

2.3. Sample characterization

The crystalline phases of the samples were studied by X-ray diffraction (XRD, Rigaku, Ultima IV with D/teX Ultra) analysis equipped with Cu-Kα radiation. The lattice parameters of the materials were refined by Rietveld analysis using an integrated X-ray powder diffraction software package PDXL (Rigaku, Version 1.3.0.0). The particle surface morphology was examined by field emission scanning electron microscopy (FE-SEM, Hitachi, S4500) operated at 8 kV. The interior structure of the $LiCoPO_4$/C nanocomposite particles was observed by using transmission electron microscopy (TEM, JEOL Ltd., JEM-2010F) equipped with energy dispersive spectroscopy (EDS) analysis. The specific surface area was determined by the Brunauer–Emmet–Teller method (BET, Shimadzu, Flow Sorb II 2300). The carbon content of $LiCoPO_4$/C nanocomposites after annealing was confirmed using an element analyzer (Yanaco, CHN corder MT-6). The thermal decomposition behavior of the as-prepared samples was determined by a Rigaku Thermo Plus thermogravimetry (TG)–differential thermal analysis (DTA) 8120 apparatus at the following conditions: heating rate; 10 °C min^{-1}, atmosphere; dry He, flow rate; 150 ml min^{-1}.

2.4. Electrochemical measurements

The electrochemical performance of $LiCoPO_4$/C nanocomposites was investigated using coin-type cells (CR2032). The cell is composed of a lithium metal negative electrode and a $LiCoPO_4$/C composite positive electrode that were separated by a microporous polypropylene film. 1 mol dm^{-3} solution of $LiPF_6$ in a mixed solvent of ethylene carbonate (EC) and dimethyl carbonate (DMC) with 1:1 in volume ratio (Tomiyama Pure Chemical Co., Ltd.) was used as the electrolyte. The cathode is comprised of 70 wt.% $LiCoPO_4$, 10 wt.% polyvinylidene fluoride (PVdF) as a binder and 20 wt.% acetylene black, which includes the acetylene black in the $LiCoPO_4$/C nanocomposites. These materials were dispersed in 1-methyl-2-pyrrolidinone (NMP). The resultant slurry was spread uniformly onto an aluminum foil using the doctor blade technique and then dried in a vacuum oven for 4 h at 110 °C. The cathode was punched into circular discs and then scraped in order to standardize the area of cathode (1 cm^2). The cell was assembled inside a glove box filled with high-purity argon gas (99.9995% purity). The cells were tested galvanostatically between 2.5 and 5.1 V versus Li^+/Li on multi-channel battery testers (Hokuto Denko, HJ1010mSM8A) at various charge/discharge rates ranging from 0.05 to 20 C (1 C = 167 mAh g^{-1}). Current densities and specific capacities were calculated on the basis of the weight of $LiCoPO_4$ in the cathode.

Cyclic voltammetry was performed using a Solartron 1255B frequency response analyzer connected to a Solartron SI 1287 electrochemical interface. The voltage ranged between 2.5 and 5.1 V at a scanning rate of 0.05 mV s^{-1}. All electrochemical measurements were performed at room temperature.

3. Results and discussion

3.1. Material characterization

Fig. 1 shows the XRD patterns of $LiCoPO_4$/C composites. For the purpose of comparison, those of as-prepared sample by SP were also shown in the figure. At a low SP temperature of 300 °C, the amorphous sample with some unidentified impurity phases could be obtained. This fact indicates that the thermal decomposition of precursor compounds is not completed and crystallization does not occur in SP process. It could be also confirmed by the thermal decomposition analysis of the as-prepared sample, which showed approximately 22% of weight loss after heating up to 600 °C (the weight loss mainly occurred at around 500 °C). On the contrary, the $LiCoPO_4$/C composite sample is the single phase of olivine structure indexed by orthorhombic *Pmna* (JCPDS 00-000-1809). The lattice parameters of $LiCoPO_4$/C composites (a = 10.2062, b = 5.9224, c = 4.7003) obtained from Rietveld refinement are in good agreement with the reported data [18,24,30,32–34].

The observation of particle morphology was done by FE-SEM. Fig. 2 presents the SEM image and particle size distribution of $LiCoPO_4$/C composites, respectively. The particle size distribution measurement as well as the calculations of the geometric mean diameter $d_{g,p}$ and the geometric standard deviation σ_g were described elsewhere [38]. The $LiCoPO_4$/C composites have much

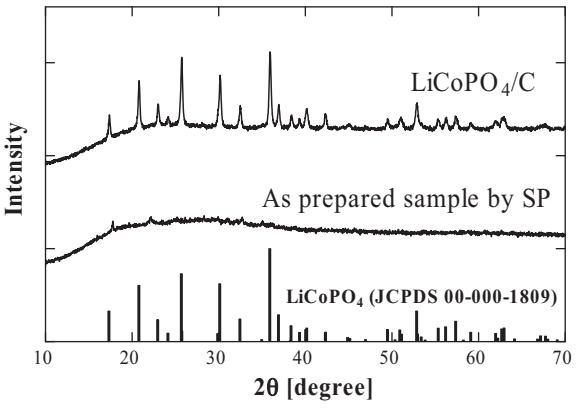

Fig. 1. XRD patterns of the as-prepared powder by SP and $LiCoPO_4$/C nanocomposites.

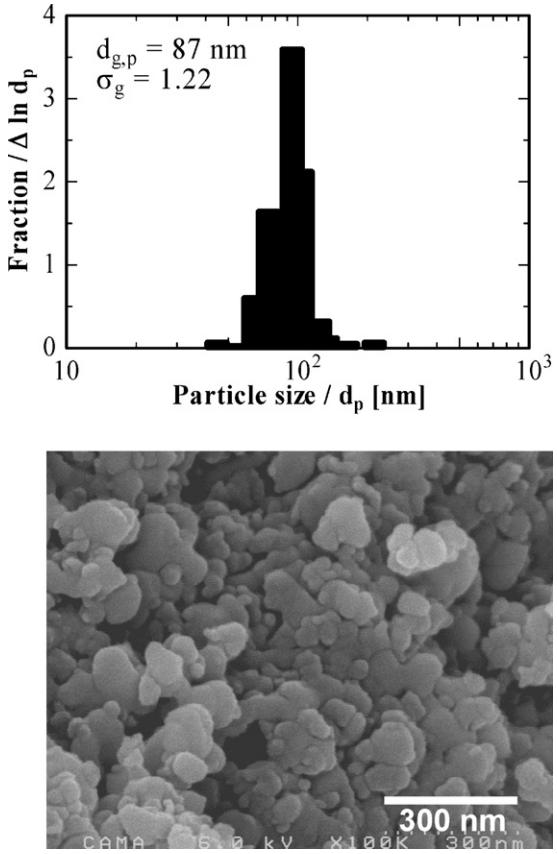

Fig. 2. SEM image and particle size distribution of $LiCoPO_4$/C nanocomposites.

small primary particle size with the geometric mean diameter $d_{g,p}$ = 87 nm and narrow particle size distribution (σ_g = 1.22). As a result, the specific surface area of $LiCoPO_4$/C composites was 41 $m^2\,g^{-1}$. The smaller primary particle size could reduce the diffusion pathway of lithium ion within the bulk material, thus enhance the ionic diffusivity of the cathode. Moreover, from TEM observation of $LiCoPO_4$/C composites, the carbon and $LiCoPO_4$ phases could be clearly observed in Fig. 3a and could be identified by EDS analysis, as shown in Fig. 3b. Therefore, it can be concluded that the $LiCoPO_4$/C nanocomposites can be successfully prepared by the present method.

3.2. Electrochemical performance

Fig. 4 shows the cyclic voltammogram of 2nd cycle for the cell containing $LiCoPO_4$/C nanocomposites as active cathode materials. The profile shows two oxidation peaks at about 4.8 and 4.9 V versus Li^+/Li, while only one reduction peak is observed at about 4.7 V. Similar cyclic voltammograms were reported by other researchers, apparently indicating a two-step mechanism of lithium deintercalation [6,7,12,21,22]. However, the reason of this phenomenon remained unclear. The only conclusion has been made so far that the two-step character of lithium extraction from $LiCoPO_4$ is an intrinsic property of this compound and could not be ascribed to the irreversible side reactions [21]. In fact, Wolfenstine et al. [39] suggested that the electrochemical oxidation behavior of $LiCoPO_4$ is different from those of $LiFePO_4$ and $LiMnPO_4$. The peak intensity of $LiCoPO_4$/C nanocomposites is higher than that of $LiCoPO_4$.

Fig. 5 presents the first discharge profile of the cells containing $LiCoPO_4$/C nanocomposites as active cathode materials at 0.1 C. For the purpose of comparison, the first discharge profile of the cells containing $LiCoPO_4$ is also shown in the figure. The $LiCoPO_4$/C nanocomposite cathode exhibited a wide and flat voltage plateau at around 4.75 V versus Li^+/Li. As expected from Fig. 4, the $LiCoPO_4$/C nanocomposite cathode delivered larger discharge capacity (141 mAh g^{-1}) in comparison with the one of $LiCoPO_4$ (94 mAh g^{-1}).

The coulomb efficiencies versus cycle number for $LiCoPO_4$/C nanocomposites at 0.1 and 1 C rate are shown in Fig. 6. The cells exhibited low coulomb efficiencies of 55 and 63% in correspondence to 0.1 and 1 C at first cycle, respectively. These might indicate that a large capacity loss occurred in the first charge–discharge process. The large irreversible capacity loss might be due to the side reactions between electrolyte and electrode, which forms the solid–electrolyte interface (SEI) on the electrode. It might lead to electrolyte oxidation and lithium loss. However, after 4 cycles, the coulomb efficiencies increase up to 80% at 0.1 C and 88% at 1 C, and become stable. After several cycles, the SEI becomes stable, which may partly eliminate the side reactions. The coulomb efficiencies at 1 C are higher than those at 0.1 C in each cycle. This reason can be explained by the result of Smith et al. [40] which the charge–discharge time is the dominant contributor to the coulomb inefficiency of Li-ion batteries cycled at low charge–discharge rates. Good coulomb efficiencies of 88% at 0.1 C and 95% at 1 C could be seen after 40 cycles.

The rate capabilities of the cells containing $LiCoPO_4$ and $LiCoPO_4$/C nanocomposites are presented in Fig. 7. The cells containing $LiCoPO_4$ exhibited first discharge capacities of 99, 94, 78, 53 and 11 mAh g^{-1} at 0.05, 0.1, 1, 5 and 20 C, respectively, while the cells containing $LiCoPO_4$/C nanocomposites delivered first discharge capacities of 142, 141, 137, 128 and 109 mAh g^{-1} at 0.05. 0.1, 1, 5 and 20 C, respectively.

Fig. 8 shows the first, second and fifth charge–discharge profiles of the cells containing $LiCoPO_4$/C nanocomposites at various charge–discharge rates of 0.1 C, 1 C and 20 C. The polarization loss is small at 0.1 and 1.0 C rate, while the irreversible capacities are very large, as predicted from Fig. 6. However, the polarization loss becomes larger and the discharge capacity gradually decrease with increasing of C-rates up to 20 C due to the slow diffusion of Li ions. Furthermore, the irreversible capacity loss in the first charge–discharge process becomes smaller in increasing of C-rate up to 20 C.

Fig. 9 shows the cycleability of the cells containing $LiCoPO_4$/C nanocomposites at 0.1 C. The discharge capacity of the $LiCoPO_4$/C nanocomposites gradually decreased with cycle number. The capacity retentions were 87% after 40 cycles. Even though this cycleability is much better compared with reported data (Table 1), the cycleability is poor in comparison with $LiMnPO_4$/C nanocomposites [37]. The capacity retention is dependent on the structure stability with lithium intercalation and deintercalation [27] and electrolyte stability [12]. Since $LiCoPO_4$ has quite small struc-

Table 1
Comparison of electrochemical performance of $LiCoPO_4$/C nanocomposites of this study and previous reported data at room temperature.

Samples	C rate	Cutoff voltages [V]	First discharge capacity [mAh g^{-1}]	Discharge capacity retention [%] (25 cycles)
This study	0.1 C	2.5–5.1	141	90
This study	20 C	2.5–5.1	109	–
Ref. [2]	0.1 C	3.0–5.3	70	–
Ref. [7]	0.17 C	3.5–5.1	100	27
Ref. [10]	0.1 C	3.0–5.1	144	55
Ref. [10]	20 C	3.0–5.1	71	–
Ref. [24]	0.05 C	3.5–5.2	108	–
Ref. [27]	0.1 C	3.0–5.0	95	32

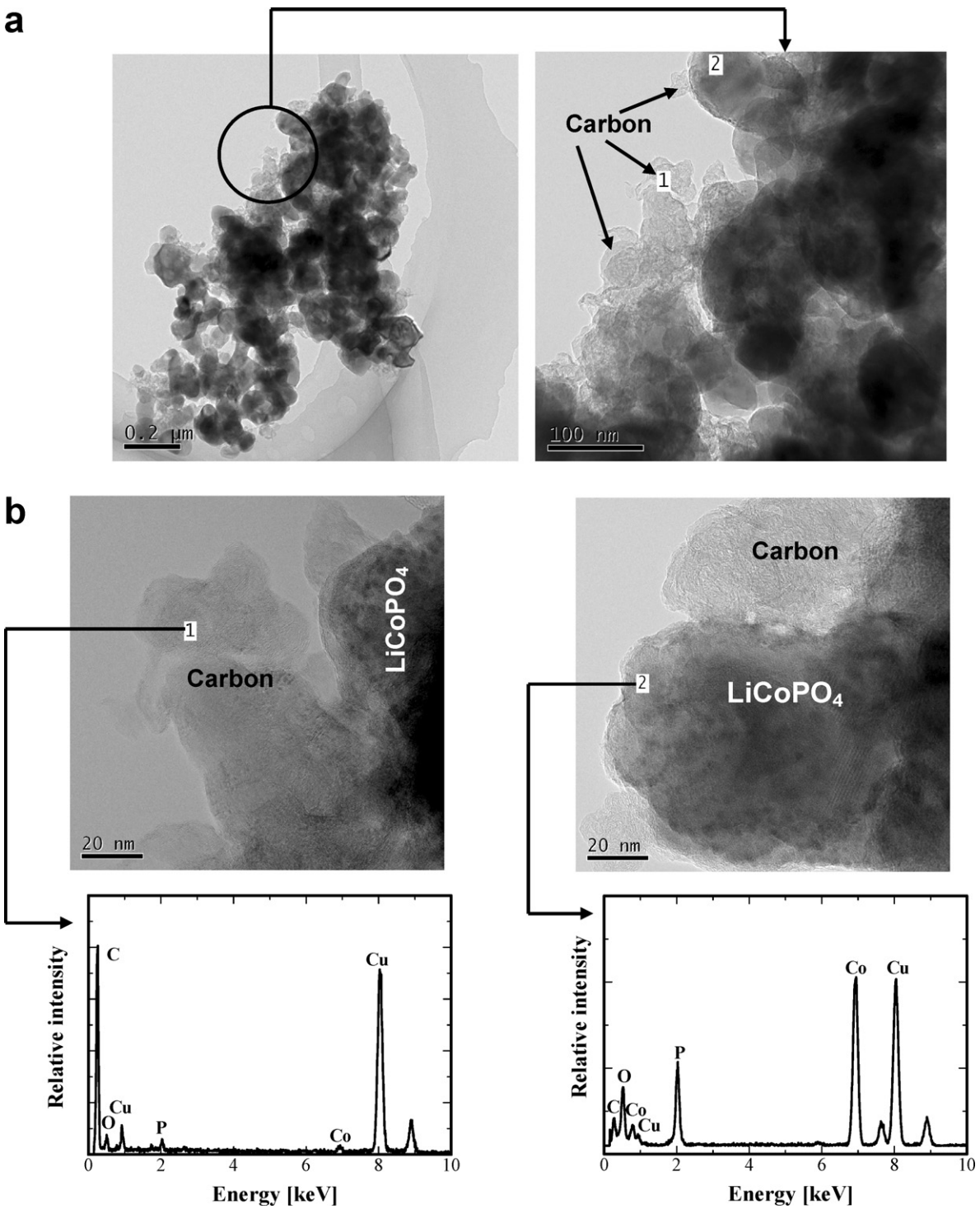

Fig. 3. (a) TEM images of the $LiCoPO_4$/C nanocomposites and (b) EDS spectrum of the $LiCoPO_4$/C nanocomposites.

ture volume change of about 2% [6] which may lead to a more stable structure for lithium insertion/extraction in comparison with $LiFePO_4$ or $LiMnPO_4$, the reason for capacity fading here may be mainly come from the electrolyte decomposition in high operation voltage. This fact has been also reported by Amine et al. [2].

Table 1 gives the comparison of $LiCoPO_4$/C nanocomposites prepared in this study with previous works, which clearly indicates that the $LiCoPO_4$/C nanocomposite is one of the best $LiCoPO_4$ cathode active materials ever reported. The excellent rate capability reported hereby could be explained based on the nanosize pathway of lithium ion, good contact between carbon and $LiCoPO_4$ phases in the composites as well as uniform chemical distribution ensured by means of SP. Moreover, the electronic conductivity of $LiCoPO_4$/C nanocomposites is almost similar to that of $LiFePO_4$/C nanocomposites, which has been reported as the cathode material with excellent rate capability [14]. Furthermore, well distribution of carbon in the nanocomposites could also contribute to better rate capability.

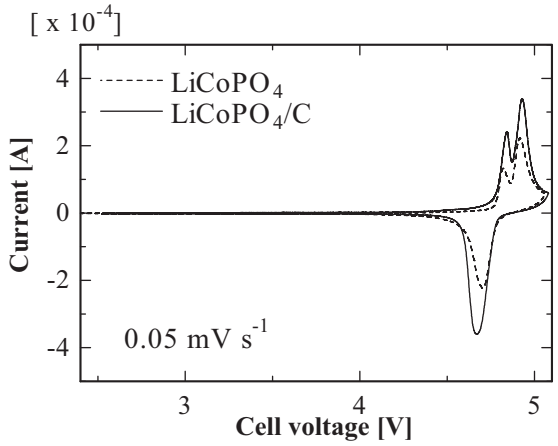

Fig. 4. Cyclic voltammograms of 2nd cycle for the cells containing $LiCoPO_4$/C nanocomposites.

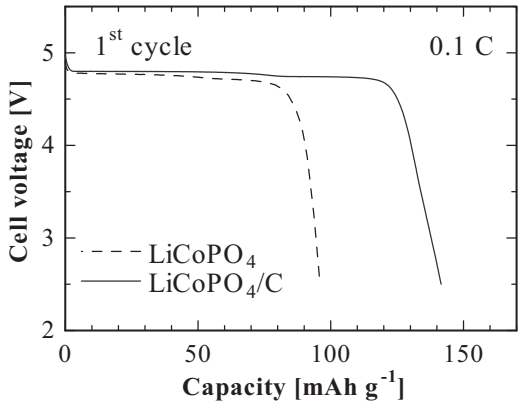

Fig. 5. First discharge profiles of the cells containing $LiCoPO_4$/C nanocomposite cathode at 0.1 C.

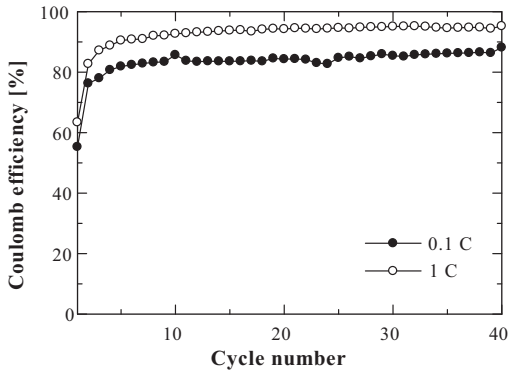

Fig. 6. Coulomb efficiency versus cycle number for $LiCoPO_4$/C nanocomposites cathode at 0.1 and 1 C.

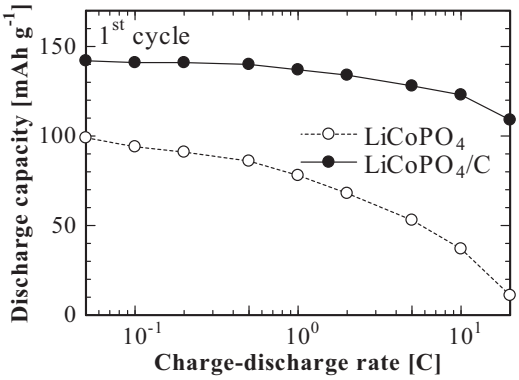

Fig. 7. Rate capabilities of the cells containing $LiCoPO_4$/C nanocomposite cathode.

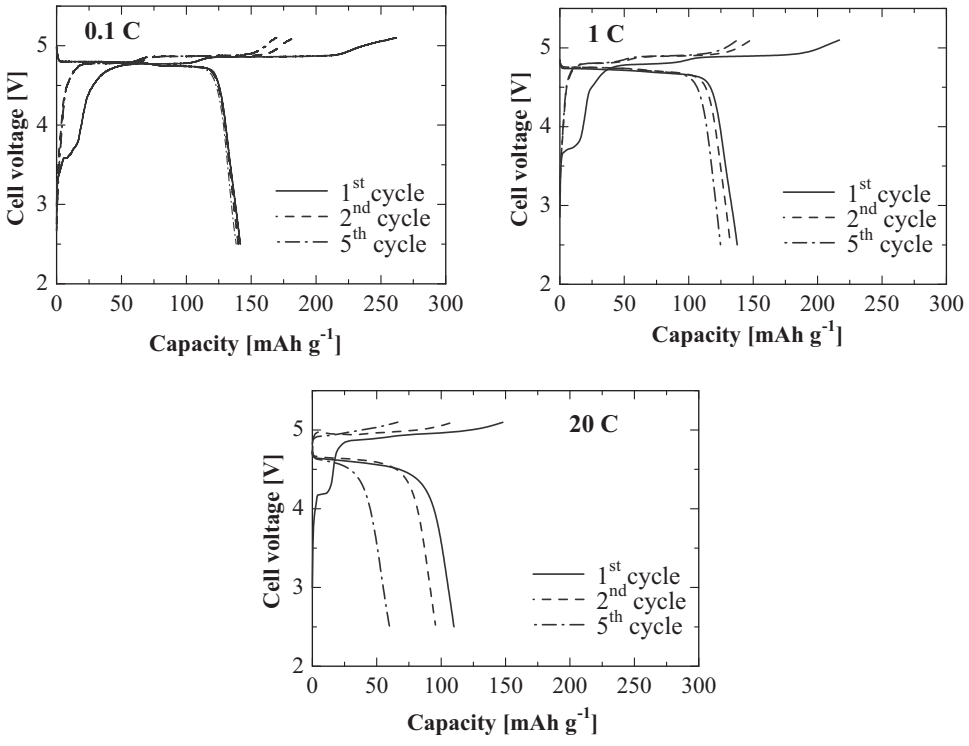

Fig. 8. Charge/discharge profiles of the cells containing $LiCoPO_4$/C nanocomposite cathode at 0.1 C, 1 C and 20 C.

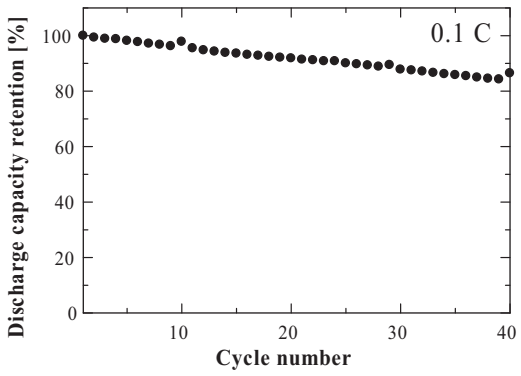

Fig. 9. Cycle performance of the cells containing $LiCoPO_4$/C nanocomposite cathode.

4. Conclusions

$LiCoPO_4$/C nanocomposites could be successfully prepared by a combination of SP and WBM followed by heat treatment in a N_2 + 3% H_2 atmosphere. The XRD patterns of $LiCoPO_4$/C nanocomposites could be identified as single phase of olivine structure indexed by orthorhombic *Pmna*. The calculated lattice parameters were well agreed with the reported data. It could also be observed from SEM and TEM images that the final samples were the $LiCoPO_4$/C nanocomposites comprise of primary particles about 100 nm in size. The $LiCoPO_4$/C nanocomposites were used as cathode materials for lithium batteries, and electrochemical performance was investigated using the Li|1 M $LiPF_6$ in EC:DMC = 1|$LiCoPO_4$/C cells at room temperature. In the cutoff voltage range from 2.5 to 5.1 V, the cells exhibited initial discharge capacities of 142, 141, 137, 128 and 109 mAh g^{-1} at 0.05, 0.1, 1, 5 and 20 C, respectively. This is among the highest rate performances have ever been reported, with significant improvement of cycleability. However, the discharge capacity still decreased with cycle number. Discharge capacity retention was 87% after 40 cycles at 0.1 C. It can be concluded that the material may have good potential for practical application if a more stable electrolyte at high voltage is developed.

Acknowledgements

The authors are grateful to the staff members (Mr. A. Hori and Mr. J. Koki) of the Center for Advanced Materials Analysis (Tokyo Institute of Technology, Japan) for the TEM observations of the samples.

References

[1] A.K. Padhi, K.S. Nanjundaswamy, J.B. Goodenough, J. Electrochem. Soc. 144 (1997) 1188–1194.
[2] A. Amine, H. Yasuda, M. Yamachi, Electrochem. Solid State Lett. 3 (2003) 178–179.
[3] J. Wolfenstine, J. Power Sources 158 (2006) 1431–1435.
[4] C. Delacourt, L. Laffont, R. Bouchet, C. Wurm, J.-B. Leriche, M. Morcrette, J.-M. Tarascon, C. Masquelier, J. Electrochem. Soc. 152 (2005) A913–A921.
[5] M. Yonemura, A. Yamada, Y. Takei, N. Sonoyama, R. Kanno, J. Electrochem. Soc. 151 (2004) A1352–A1356.
[6] N.N. Bramnik, K.G. Bramnik, C. Baehtz, H. Ehrenberg, J. Power Sources 145 (2005) 74–81.
[7] N.N. Bramnik, K. Nikolowski, C. Baehtz, K.G. Bramnik, H. Ehrenberg, Chem. Mater. 19 (2007) 908–915.
[8] A. Andersson, B. Kalska, L. Häggström, J. Thomas, Solid State Ionics 130 (2000) 41–52.
[9] C. Delacourt, P. Poizot, M. Morcrette, J.-M. Tarascon, C. Masquelier, Chem. Matter. 16 (2004) 93–99.
[10] H.H. Li, J. Jin, J.P. Wei, Z. Zhou, J. Yan, J. Electrochem. Commun. 11 (2009) 95–98.
[11] I.C. Jang, H.H. Lim, S.B. Lee, K. Karthikeyan, V. Aravindan, K.S. Kang, W.S. Yoon, W.I. Cho, Y.S. Lee, J. Alloys Compd. 497 (2010) 321–324.
[12] Z. Yujuan, W. Suijun, Z. Chunsong, X. Dingguo, Rare Met. 28 (2) (2009) 117–121.
[13] M.E. Rabanal, M.C. Gutierrez, F. Garcia-Alvarado, E.C. Gonzalo, M.E. Arroyo-de Dompablo, J. Power Sources 160 (2006) 523–528.
[14] M. Konarova, I. Taniguchi, J. Power Sources 195 (2010) 3661–3667.
[15] M. Konarova, I. Taniguchi, Powder Technol. 191 (2009) 111–116.
[16] J. Yang, J.J. Xu, J. Electrochem. Soc. 153 (2006) A716–A723.
[17] M. Piana, M. Arrabito, S. Bodoardo, A. D'Epifanio, D. Satolli, F. Croce, B. Scrosati, Ionics 8 (2002) 17–26.
[18] D. Wang, Z. Wang, X. Huang, L. Chen, J. Power Sources 146 (2005) 580–583.
[19] R. Ruffo, C.M. Mari, F. Morazzoni, F. Rosciano, R. Scotti, Ionics 13 (2007) 287–291.
[20] J. Wolfenstine, J. Read, J.L. Allen, J. Power Sources 163 (2007) 1070–1073.
[21] M. Nakayama, S. Goto, Y. Uchimoto, M. Wakihara, Y. Kitajima, Chem. Matter. 16 (2004) 3399–3401.
[22] N.N. Bramnik, K.G. Bramnik, T. Buhrmester, C. Baehtz, H. Ehrenberg, H. Fuess, J. Solid State Electrochem. 8 (2004) 558–564.
[23] B. Jin, H.-B. Gu, K.-W. Kim, J. Solid State Electrochem. 12 (2008) 105–111.
[24] D.-W. Han, Y.-M. Kang, R.-Z. Yin, M.-S. Song, H.-S. Kwon, Eletrochem. Commun. 11 (2009) 137–140.
[25] V. Grigorova, D. Roussev, P. Deniard, S. Jobic, J. Phys. Chem. Solids 66 (2005) 1598–1608.
[26] J. Wolfenstine, U. Lee, B. Poese, J.L. Allen, J. Power Sources 144 (2005) 226–230.
[27] M.V.V.M. Satya Kishore, U.V. Varadaraju, Mater. Res. Bull. 40 (2005) 1705–1712.
[28] F. Wang, J. Yang, Y. NuLi, J. Wang, J. Power Sources 195 (2010) 6884–6887.
[29] X. Huang, J. Ma, P. Wu, Y. Hu, J. Dai, Z. Zhu, H. Chen, H. Wang, Mater. Lett. 59 (2005) 578–582.
[30] Gangulibabu, D. Bhuvaneswari, N. Kalaiselvi, N. Jayaprakash, P. Periasamy, J. Sol–Gel Sci. Technol. 49 (2009) 137–144.
[31] P. Deniard, A.M. Dulac, X. Rocquefelte, V. Grigorova, O. Lebacq, A. Pasturel, S. Jobic, J. Phys. Chem. Solids 65 (2004) 229–233.
[32] H. Ehrenberg, N.N. Bramnik, A. Senyshyn, H. Fuess, Solid State Sci. 11 (2009) 18–23.
[33] D. Sahnmukaraj, R. Murugan, Ionics 10 (2004) 88–92.
[34] R. Saint-Martin, S. Franger, J. Cryst. Growth 310 (2008) 861–864.
[35] J. Xie, N. Imanishi, T. Zhang, A. Hirano, Y. Takeda, O. Yamamoto, J. Power Sources 192 (2009) 689–692.
[36] J.L. Shui, Y. Yu, X.F. Yang, C.H. Chen, Electrochem. Commun. 8 (2006) 1087–1091.
[37] T.N.L. Doan, I. Taniguchi, J. Power Sources 196 (2011) 1399–1408.
[38] I. Taniguchi, Mater. Chem. Phys. 92 (2005) 172–179.
[39] J. Wolfenstine, B. Poese, J.L. Allen, J. Power Sources 138 (2004) 281–282.
[40] A.J. Smith, J.C. Burns, J.R. Dahn, Electrochem. Solid State Lett. 13 (2010) A177–A179.